Supporting Information

Flux Synthesis of Layered Oxyhalide Bi_4NbO_8Cl Photocatalyst for Efficient Z-scheme Water Splitting Under Visible Light

Kanta Ogawa,[a] Akinobu Nakada,[a] Hajime Suzuki,[a,†] Osamu Tomita,[a] Masanobu Higashi,[a] Akinori Saeki,[b] Hiroshi Kageyama,[a,c,] Ryu Abe[a,c,*]*

a. Department of Energy and Hydrocarbon Chemistry, Graduate School of Engineering, Kyoto University, Nishikyo-ku, Kyoto, 615-8510, Japan

b. Department of Applied Chemistry, Graduate School of Engineering, Osaka University, 2-1 Yamadaoka, Suita, Osaka 565-0871, Japan

c. JST-CREST, Japan Science and Technology Agency (JST), Kawaguchi, Saitama 332-0012, Japan

[*]Email: kage@scl.kyoto-u.ac.jp, ryu-abe@scl.kyoto-u.ac.jp

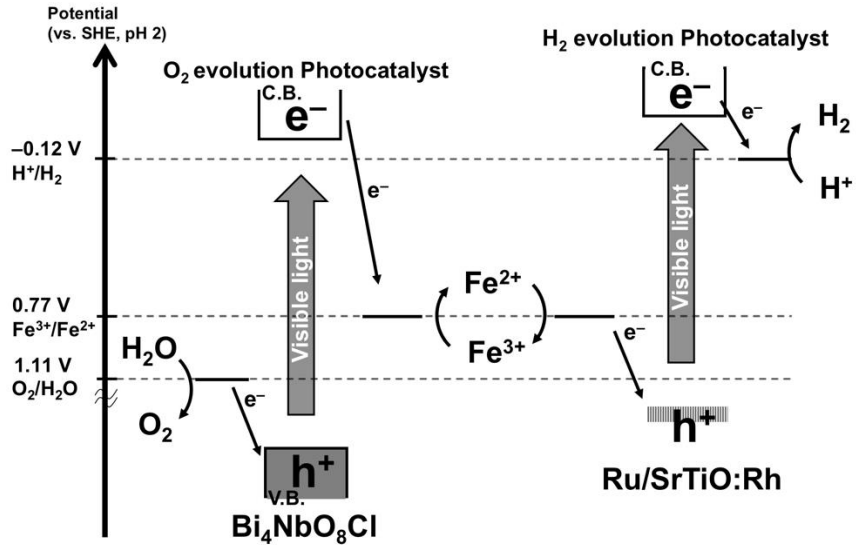

Figure S1. The schematic energy diagram of the Z-scheme water splitting system composed of Bi_4NbO_8Cl, $Ru/SrTiO_3$:Rh and Fe^{3+}/Fe^{2+} redox.

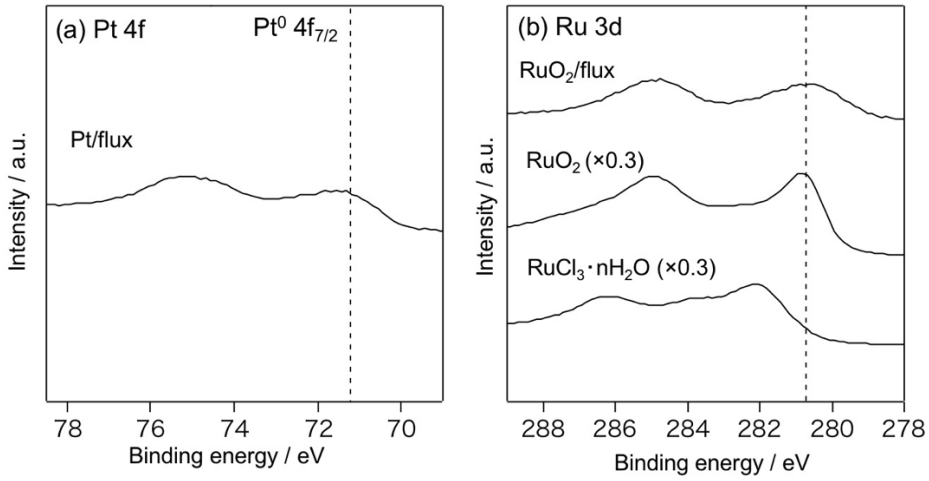

Figure S2. XP spectra of (a) Pt 4f and (b) Ru 3d region of Pt or Ru species loaded Bi_4NbO_8Cl samples prepared via the flux method (CsCl/NaCl flux at 650 °C), along with those of commercial RuO_2 (Wako Pure Chemical Industries, Ltd.) and $RuCl_3 \cdot nH_2O$ (Wako Pure Chemical Industries, Ltd) as references for comparison. Each cocatalyst was loaded via impregnation followed by heating under H_2 flow (20 mL min^{-1}) at 150 °C for Pt or Ar flow (20 mL min^{-1}) at 450 °C for RuO_2. The binding energy of Pt^0 was referred to a reference hand book.[1]

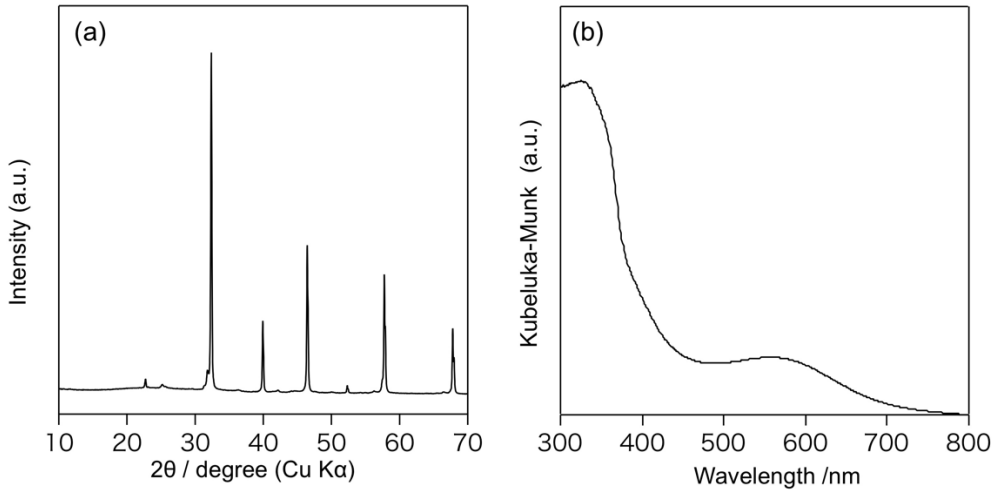

Figure S3. (a) XRD pattern and (b) DRS of as-prepared $SrTiO_3$:Rh.

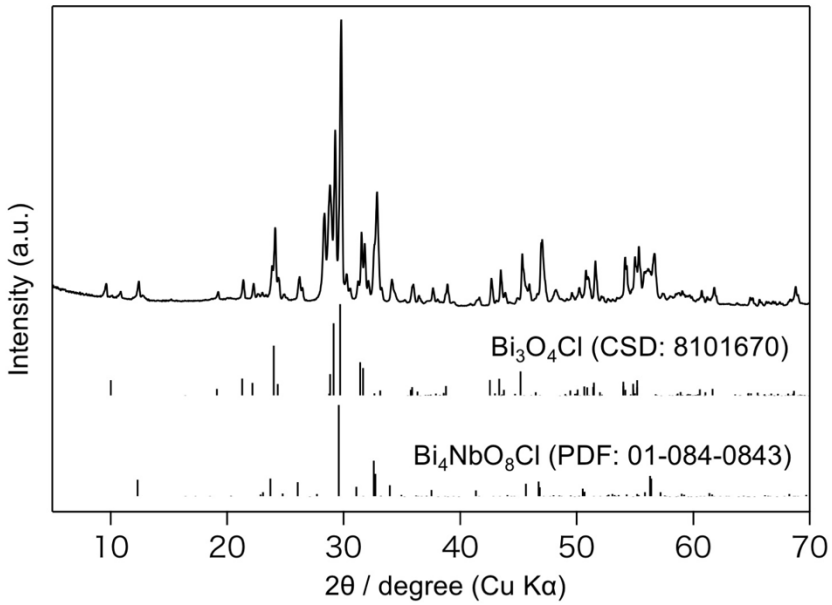

Figure S4. XRD patterns of Bi_4NbO_8Cl prepared by calcination of the mixture of the materials in air at 650 °C without any flux.

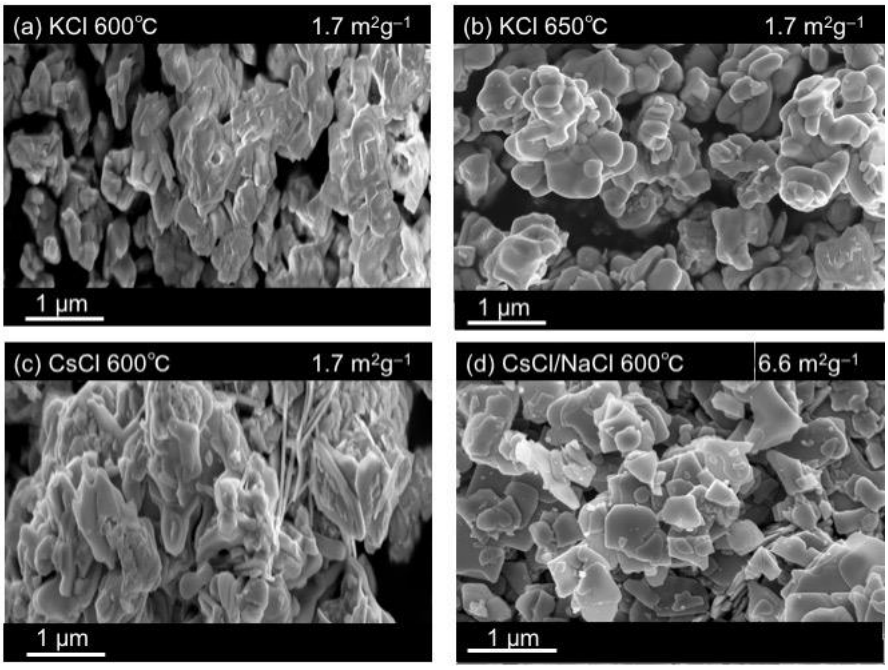

Figure S5. SEM images of Bi_4NbO_8Cl prepared via the flux method (a,b) with KCl at 600 and 650 °C; (c) with CsCl at 600 °C; (d) with CsCl/NaCl at 600 °C.

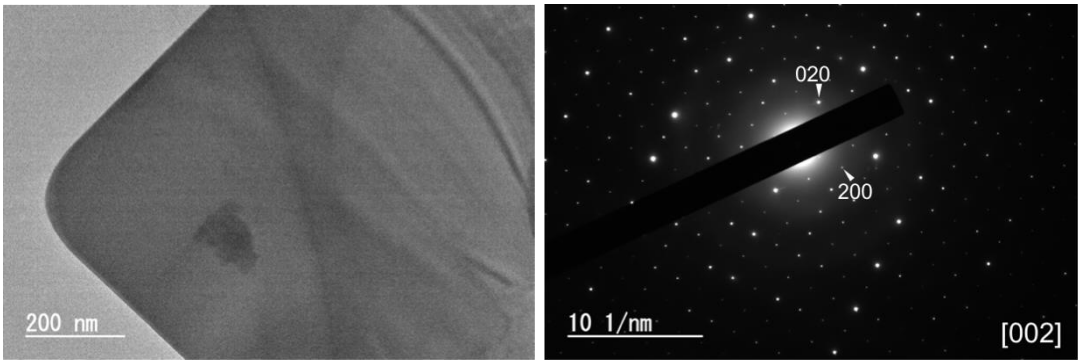

Figure S6. TEM image and electron diffraction patterns of Bi_4NbO_8Cl prepared via the flux method (CsCl/NaCl flux at 650 °C).

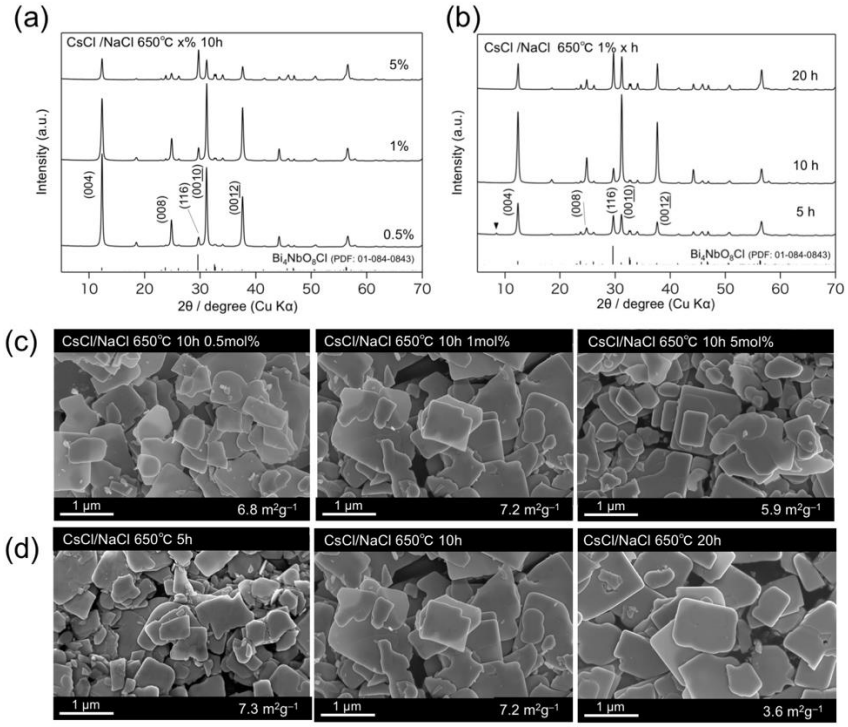

Figure S7. (a,b) XRD patterns and (c,d) SEM images of Bi_4NbO_8Cl prepared with CsCl/NaCl flux at various solute concentrations and calcination times.

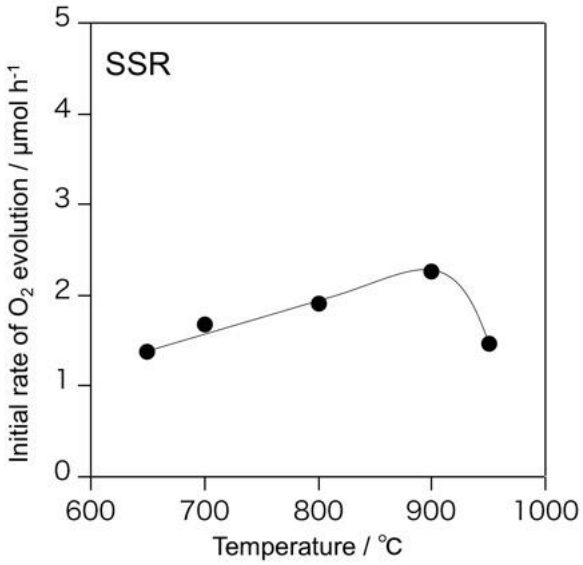

Figure S8. Initial rates of O_2 evolution over Bi_4NbO_8Cl samples prepared at various temperature (650 ~ 950 °C) via the solid-state reaction method in an aqueous $FeCl_3$ solution (8 mM, 100 mL) under visible light irradiation ($\lambda > 400$ nm).

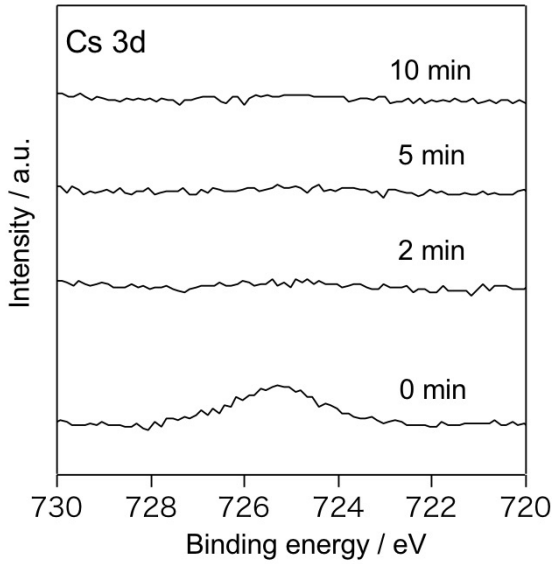

Figure S9. XP spectra of Cs 3d region of the flux sample before and after Ar sputtering (2, 5, 10 min). The binding energies were referenced to the Au $4f_{7/2}$ level of deposited Au metal.

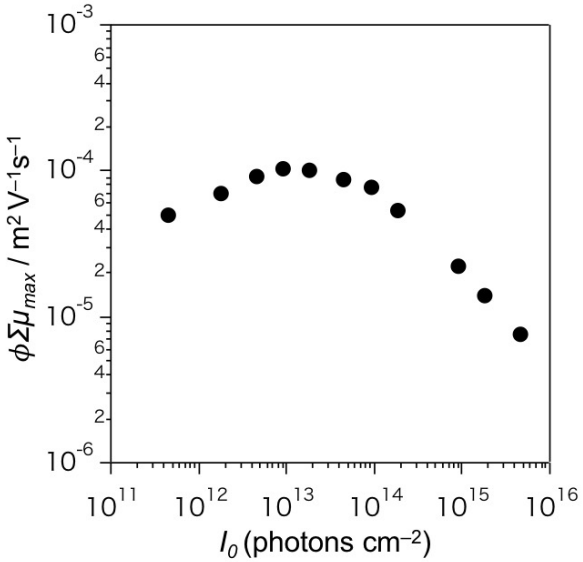

Figure S10. Dependence of $\phi\sum\mu_{max}$ on the incident laser intensity (I_0) of the flux sample. The initial increase of $\phi\sum\mu_{max}$ with increasing I_0 is due to a trap filling effect (an increase and saturation of $\sum\mu$), while the gradual decrease at high I_0 is rationalized by a high order deactivation process such as exciton−exciton annihilation, exciton−carrier annihilation, and charge recombination, which occur within the time resolution.[2,3]

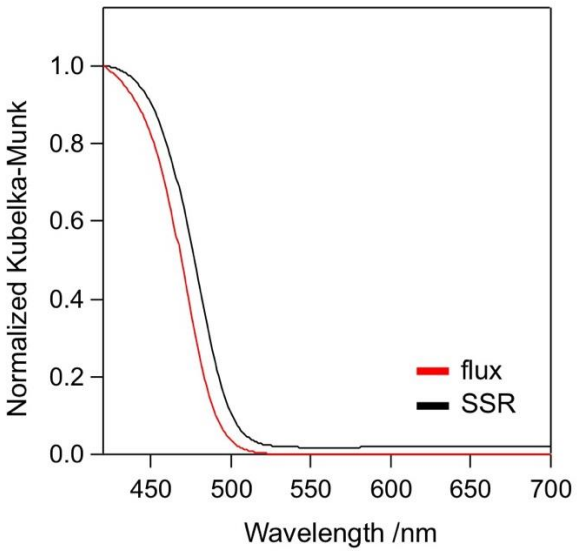

Figure S11. DRS of Bi_4NbO_8Cl samples prepared via the flux method (CsCl/NaCl flux at 650 °C) and the solid-state reaction method.

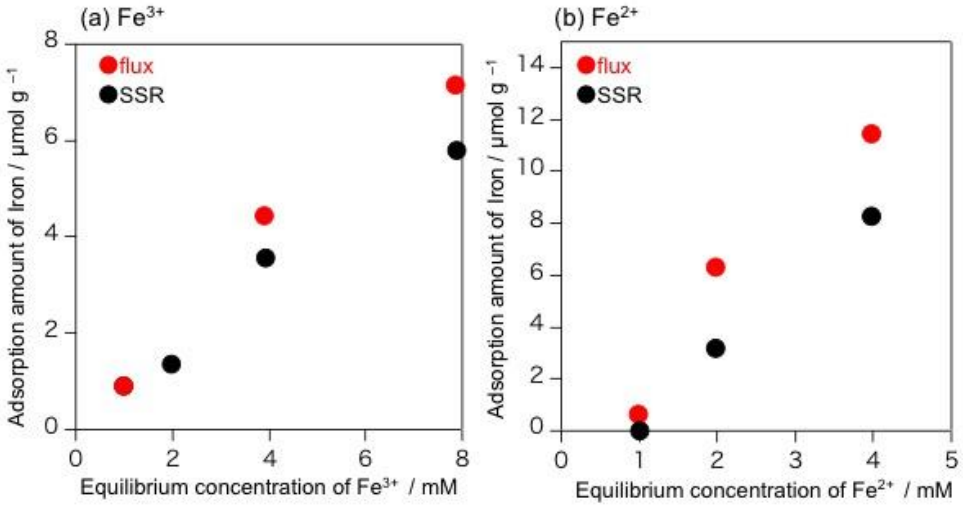

Figure S12. Adsorption properties of (a) Fe^{3+} and (b) Fe^{2+} ions on the Bi_4NbO_8Cl samples prepared via the flux method (CsCl/NaCl flux at 650 °C) and the solid-state reaction method.

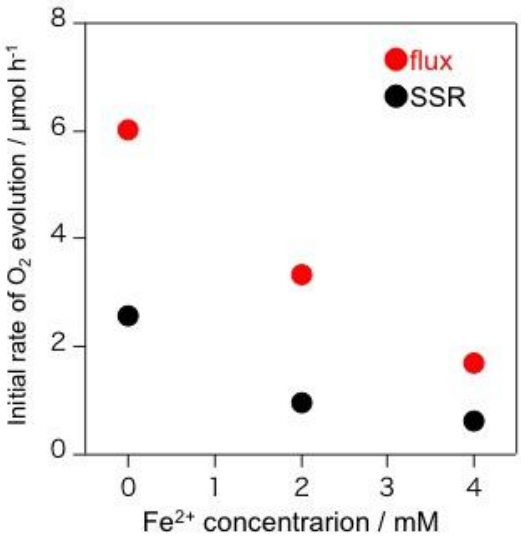

Figure S13. Initial rates of O_2 evolution over Bi_4NbO_8Cl samples prepared via the flux method (CsCl/NaCl flux at 650 °C) and the solid-state reaction method in an solution containing different concentrations of Fe^{2+} (0 ~ 4 mM) and a fixed concentration of Fe^{3+} (8 mM, 100 mL) under visible light irradiation (λ > 400 nm).

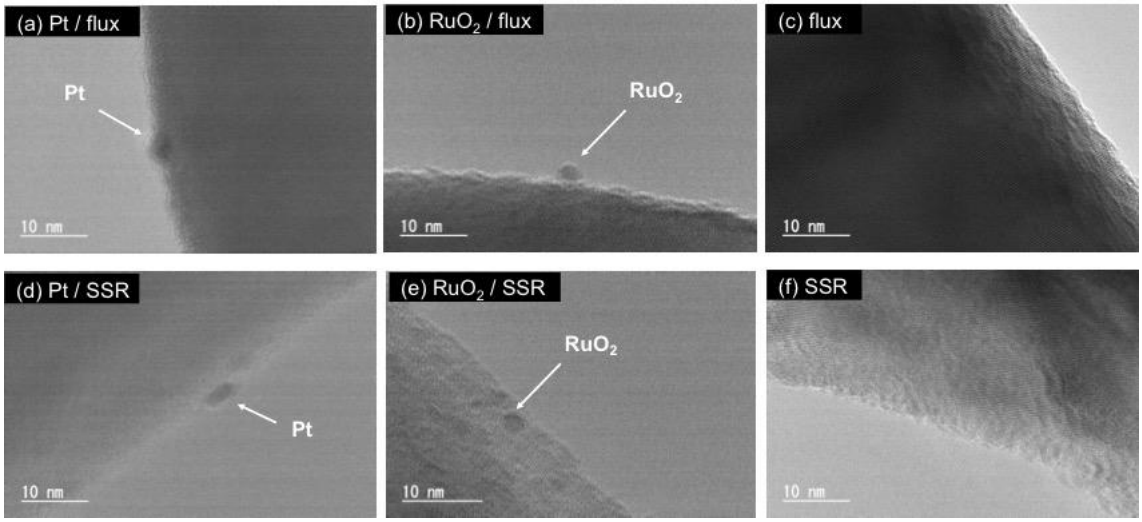

Figure S14. TEM images of (a,d) Pt- or (b,e) RuO_2-loaded Bi_4NbO_8Cl, along with (c,f) unmodified ones. The Bi_4NbO_8Cl samples prepared via (a-c) the flux method (CsCl/NaCl flux at 650 °C) and (d-f) the solid-state reaction method.

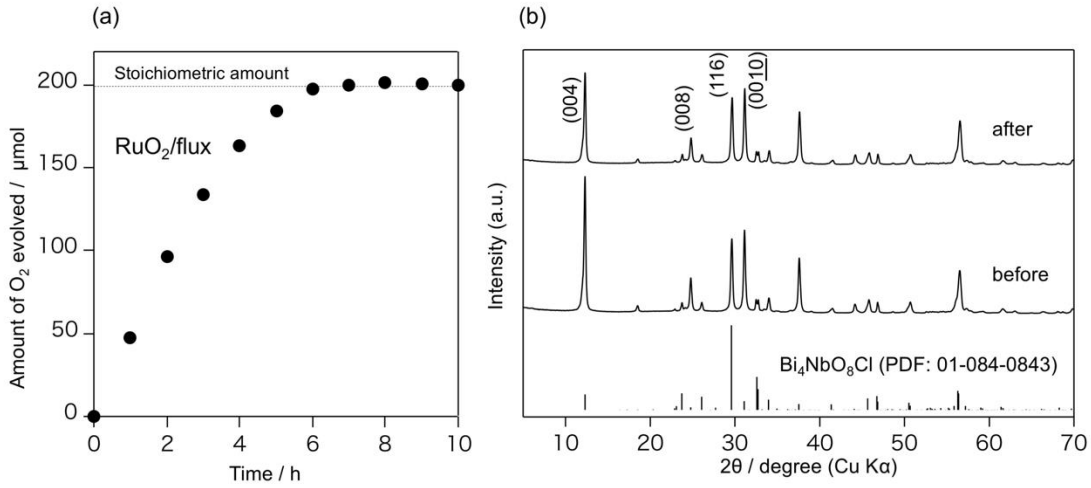

Figure S15. (a) Time course of O_2 evolution over a RuO_2-loaded Bi_4NbO_8Cl sample prepared via the flux method (CsCl/NaCl flux at 650 °C) in an aqueous $FeCl_3$ solution (8 mM, 100 mL) under visible light irradiation ($\lambda > 400$ nm). (b) XRD patterns of the RuO_2-loaded Bi_4NbO_8Cl before and after the photocatalytic reaction.

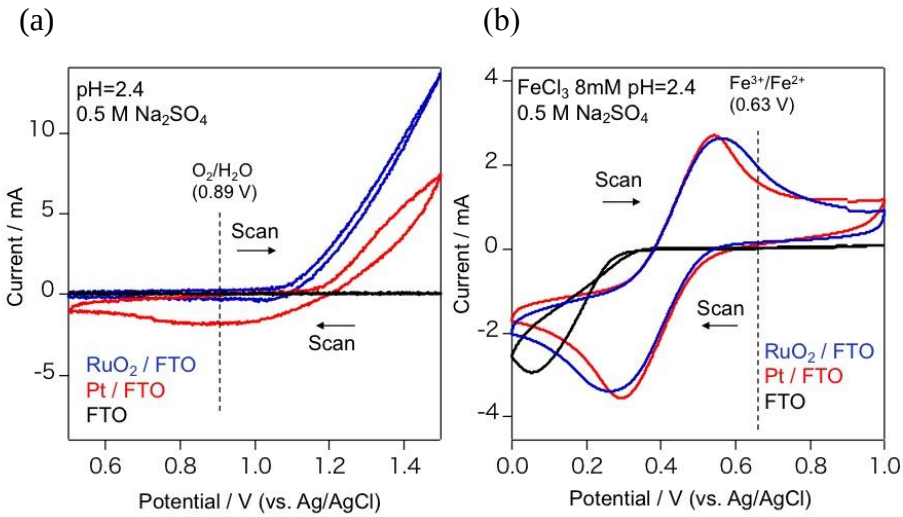

Figure S16. CV profiles of FTO substrates loaded with Pt or RuO_2 in 0.5 M aqueous Na_2SO_4 solution (a) in the absence and (b) presence of Fe^{3+} (8 mM, pH 2.4).

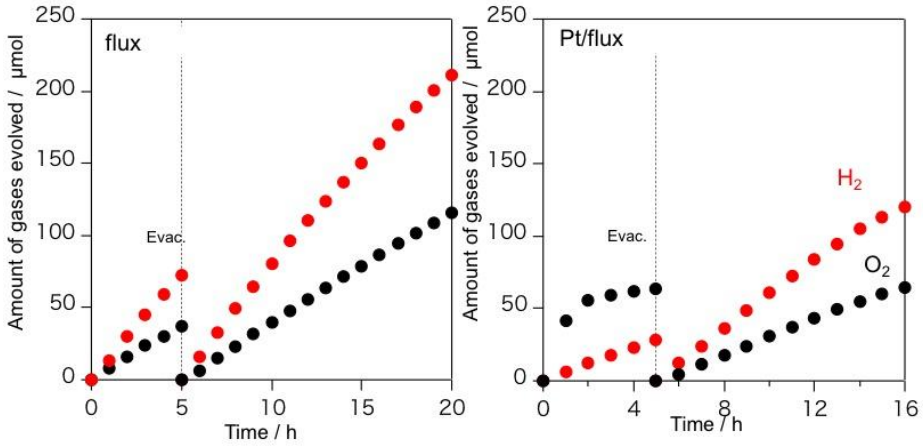

Figure S17. Time courses of H_2 and O_2 evolution over a mixture of bare or Pt-loaded Bi_4NbO_8Cl samples prepared via the flux method (CsCl/NaCl flux at 650 °C) (50 mg) and $Ru/SrTiO_3$:Rh (50 mg) in $FeCl_3$ aqueous solution (2 mM, 100 mL) at pH 2.4 under visible light irradiation ($\lambda > 400$ nm).

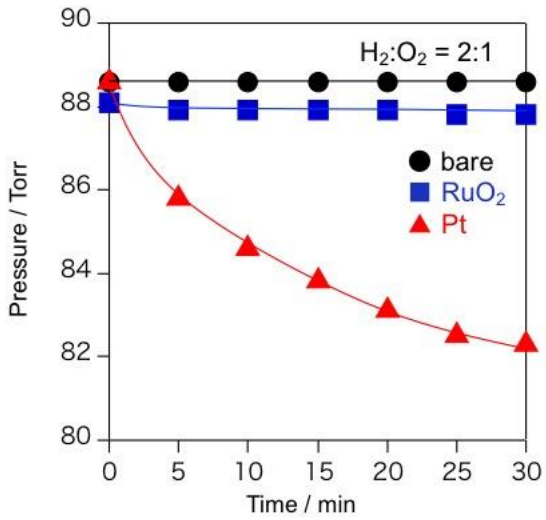

Figure S18. Water formation from H_2 and O_2 in the gas-phase reaction over Pt/flux, RuO_2/flux and flux. A mixture of H_2 and air gases (H_2 : O_2 = 2 : 1) was introduced into a gas-circulating system with a Pyrex glass cell containing 20 mg of photocatalyst powder without water.

References

(1) Jhon, F. M.; William, F. S.; Kenneth, D. B. *Handbook of X-Rays Photoelectron Spectroscopy*; Jill, C., Ed.; Perkin-Elmer Corporation: Minnesota, 1992.

(2) Kroeze, J. E.; Savenije, T. J.; Warman, J. M. Electrodeless Determination of the Trap Density, Decay Kinetics, and Charge Separation Efficiency of Dye-Sensitized Nanocrystalline TiO_2. *J. Am. Chem. Soc.* **2004**, *126*, 7608–7618.

(3) Saeki, A.; Yasutani, Y.; Oga, H.; Seki, S. Frequency-Modulated Gigahertz Complex Conductivity of TiO_2 Nanoparticles: Interplay of Free and Shallowly Trapped Electrons. *J. Phys. Chem. C* **2014**, *118*, 22561–22572.